Design of Smith-Purcell emitter in femtosecond accelerator[*]

BEI Hua(卑华)[1,2;1)]　　LIN Xu-Ling(林栩凌)[1,2]　　DAI Zhi-Min(戴志敏)[1,2]

1 (Shanghai Institute of Applied Physics, Chinese Academy of Sciences, Shanghai 201800, China)
2 (Graduate University of Chinese Academy of Sciences, Beijing 100049, China)

Abstract　Based on the femtosecond accelerator device, we are planning to build a broad band and tunable THz source using the Smith-Purcell radiation mechanism. Coherent Smith-Purcell radiation could be achieved owing to the super-short bunch produced in the device. To shorten the distance between the beam and grating, we use Transport to match the beta function producing a sheet beam on the grating surface. The optimization of grating length, groove depth and groove width are given in the paper. Then the radiation power for the shallow and deep grating using these parameters are presented. The detection devices and methods are also briefly discussed.

Key words　THz source, Smith-Purcell radiation, coherence, optimization

PACS　02.70.-c, 29.27.Eg, 41.60.-m

1　Introduction

Based on the definition by P. H. Siegel[1], the so-called Terahertz (THz) region is referred to the frequency band between 300—3000 GHz. This band contains abundant information of science but is not known to us at all. Recently, THz science and technology has been attracting considerable attention in the fields of source, detection and application research.

The THz radiation generated by the vacuum electron device is often the ring-based or linac-based source, which has some unique merits such as high emission power and brightness.

The Smith-Purcell radiation (SPR) is a new source producing THz radiation. It was first observed by S. J. Smith and E. M. Purcell[2] in 1953. They suggested that the radiation was emitted when an electron passed near the surface of a metal diffraction grating, moving perpendicular to the tooth.

The experiment device based on SPR can be designed to be compact and the radiation should be broad band and tunable. Besides, the fabrication of grating is not complicated.

Coherent Smith-Purcell radiation occurs when the wavelength is comparable to or longer than the longitudinal length of the bunch. We prefer coherent radiation to incoherent one because the power of the former is approximately proportional to the square of beam current and is enhanced by a factor N compared with the latter, where N is the number of electrons per bunch. Moreover, the coherence superiority can also be found in beam diagnostics aspect[3, 4].

The first coherent SPR was observed in LNSTU in Japan[5], and the power intensity was enhanced by several orders compared with incoherent SPR. And our research work has been done in the Femtosecond Accelerator, to produce the coherent THz radiation also based on the SP emission mechanism.

Thus, most part of this paper is concentrated on the design of coherent Smith-Purcell emitter. First, the device where our experiment will be carried on is introduced, and the operation status is given in Section 2. And in Section 3, the design results for our experiment including the beam beta function matching and the grating parameter optimization is presented in detail. Finally, the detection devices and methods are also briefly stated in Section 4.
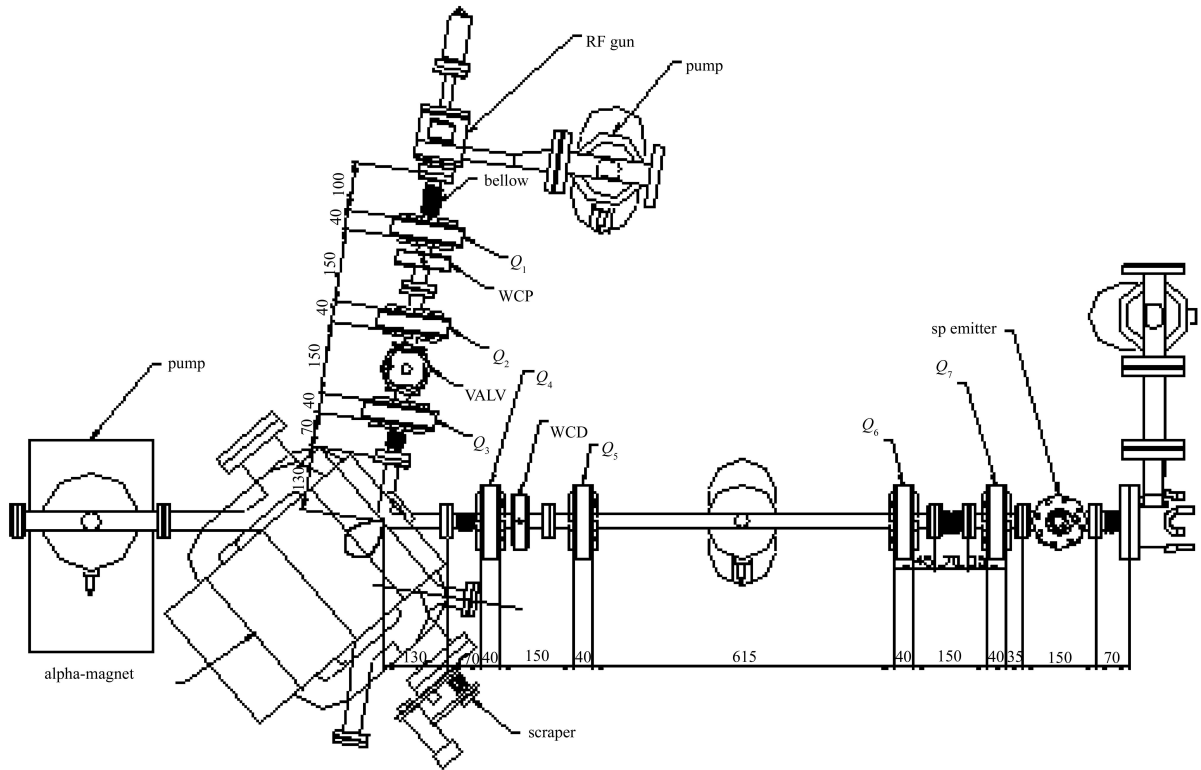
Fig. 1.   Schematic of the position where the SP emitter is placed.

2   Background of our experiment

The femtosecond accelerator is the main device in the THz Research Centre of SINAP. The coherent THz radiation with high brightness will be emitted when super-short bunches pass through the aluminum foil, undulator and bend magnets. According to the current operation status of the machine, the primary parameters for electron beam are listed in Table 1.

Table 1.   Parameters of electron beam.

beam parameters	
beam energy/MeV (maximum)	21.3
beam charge/nC	0.068
normalized emittance/mm·mrad	$\sim 10\pi$
macro-bunch repetition frequency/Hz	3.125—12.5
micro-bunch repetition frequency/MHz	2856
macro-bunch duration/μs	2—3
micro-bunch duration/fs (FWHM)	250

The Smith-Purcell emitter or SPE as an abbreviation is placed at the end of low energy transmission line and before the accelerator tube in place of the coherent transition radiation emitter, as shown in Fig. 1.

3   Design of experiment parameters

3.1   Optimization of beam parameters

The equation of radiation energy for single electron with the charge q emitted in order n per unit solid angle in direction (η, ζ) is given by Eq. (1)

$$\frac{\mathrm{d}W_n}{\mathrm{d}\Omega} = \frac{N_w q^2 |n|^2 \beta_0^3 \cos^2\eta \cos^2\zeta}{2D\varepsilon_0(1-\beta_0\sin\eta)^3}|R_n|^2 \exp\left(-\frac{z_0}{h_{\mathrm{int},n}}\right),$$
(1)

where N_w is the number of the grating periods, D is the grating period, β_0 is the relative velocity of the electron beam corresponding to the speed of light, $|R_n|^2$ is the radiation factor, z_0 is the electron-grating distance and ε_0 is the permittivity of vacuum.

$$h_{\mathrm{int},n} = \frac{D(1/\beta_0 - \sin\eta)}{4\pi|n|\sqrt{1/\beta_0^2 - 1 + \cos^2\eta\sin^2\zeta}} .$$
(2)

We can conclude from Eq. (1) that the emission energy is sensitive to the beam-grating distance. When z_0 is much large than the interaction height $h_{\mathrm{int},n}(2)$, the radiation can be ignored. Seen from Fig. 2, envelope of the electron beam develops during the passage. The distance z_0 of the electron-beam axis above the grating is defined by the requirement that its envelope just touches the grating at $x=0$ and L when the beam waist is just above the center of the grating.
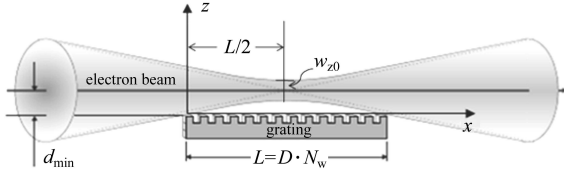
Fig. 2.   Scheme of the beam envelope development on the surface of the grating.

From the envelope equation, the vertical beam radius $w_z(x)$ could be given by[5]

$$w_z^2(x) = w_{z0}^2 + (x - L/2)^2 \cdot \frac{(\varepsilon^N/\pi)^2}{w_{z0}^2 \cdot (\beta_0\gamma_0)^2} , \qquad (3)$$

where w_{z0} is the beam waist size at $x = L/2$, ε^N is the normalized emittance and γ is the Lorentz factor. It is easier to get the minimum value of the distance

$$d_{\min} = \sqrt{\frac{L \cdot \varepsilon^N/\pi}{\beta_0\gamma_0}} ,$$

when

$$w_{z0} = \sqrt{\frac{L \cdot \varepsilon^N/\pi}{2\beta_0\gamma_0}} .$$

We first set $L=60$ mm, then we have $w_{z0}=232$ μm. As for our accelerator, we just need to adjust the strength of $Q6$ and $Q7$ quadrupoles whose maximum gradient of magnetic field is 4 T/m, located just before the position of SP emitter. The software Transport or OPA could be used to realize the beam output as what we expect.

Figure 3, 4 show us the evolvement of the beta function and the beam envelope using the Transport code. And the results are $\sigma_{z,\mathrm{rms}}=232$ μm and $\sigma_{y,\mathrm{rms}}=5.74$ mm. It is evident that the beam could be recognized as the sheet beam above the surface of the grating which is an advantage factor for SPE. And the matching results show that the gradient of magnetic field is 0.1186 T/m and -2.0699 T/m for $Q6$ and $Q7$ respectively. The same conclusion could be arrived with the OPA code.
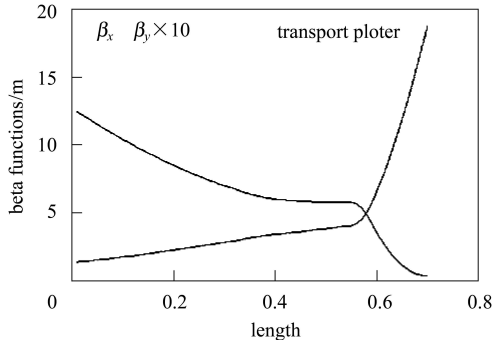

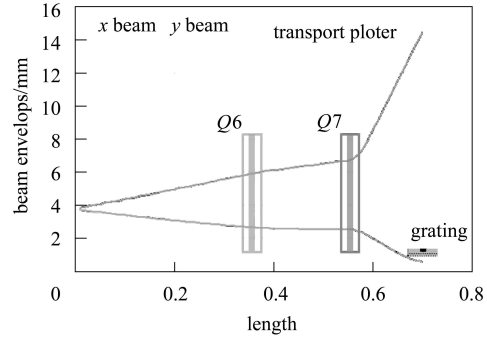Fig. 3.   Evolvement of beta function.

Fig. 4.   Scheme of the beam envelope development and the position of the quadrupoles and the grating.

3.2   Optimization of grating length

We first give the expression of the power emitted in order n by the beam with a constant current I while passing over N_w grating periods per unit solid angle in direction (ζ, η)

$$\frac{\mathrm{d}P_n}{\mathrm{d}\Omega} = \frac{IN_wq|n|^2\beta_0^3\cos^2\eta\cos^2\zeta}{2D\varepsilon_0(1-\beta_0\sin\eta)^3}|R_n|^2[S_{\mathrm{inc}}+(N-1)S_{\mathrm{coh}}],$$
$$(4)$$

where S_{inc} and S_{coh} are the incoherent factor and coherent factor respectively, which could be expressed as

$$S_{\mathrm{inc}} = \int_0^\infty \exp\left[-\frac{z}{h_{\mathrm{int},n}(\eta,\zeta)}\right]f_z(z)\mathrm{d}z ,$$
$$S_{\mathrm{coh}} = \left|\int_{-\infty}^\infty \exp(-\mathrm{i}\omega t)f_t(t)\mathrm{d}t\right|^2 \times$$
$$\left|\int_{-\infty}^\infty \exp(-\mathrm{i}\beta y)f_y(y)\mathrm{d}y\right|^2 \times \qquad (5)$$
$$\left|\int_0^\infty \exp\left[-\frac{z}{2h_{\mathrm{int},n}(\eta,\zeta)}\right]f_z(z)\mathrm{d}z\right|^2 .$$

The power calculation includes the coherent portion and the incoherent one. Fig. 5 represents that for bunch with Gaussian profile with our experiment parameters, the enhancement of the coherent portion over the incoherent one can be eight orders of magnitude higher.
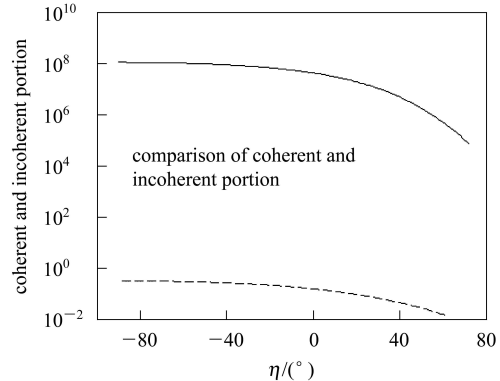

Fig. 5.   Comparison of the coherent and incoherent portions.

So we only need to consider the coherent portion in Eq. (4). For the envelope shape as Fig. 4, we can conclude that the distance varies with the grating length seen from Fig. 6. Here we adopt the same grating period 369 μm for different grating lengths, i.e. we adopt the gratings with different number of periods N_w thus in turn deciding the beam-grating distance which is also included in the calculation of the electron distribution density function f_z (see Eq. (5)). From Fig. 7, we can conclude that the longer the grating is, the stronger the intensity should be. Besides, the father the beam is away from the grating surface, the easier to realize in technical aspect. So the optimized length of the grating should be 0.06 m and the number of periods should be 160, meanwhile the beam-grating distance is set to be 360 μm.
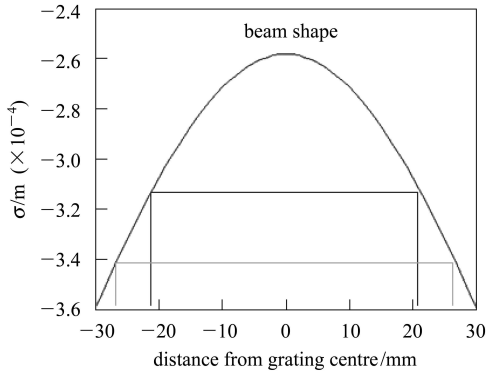

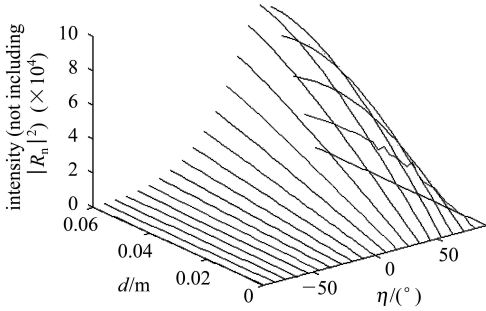Fig. 6. Relative position for the beam and the grating.

Fig. 7. Intensity without considering the radiation factor.

3.3 Optimization of groove width and depth

The most important but tough work for calculating the emission power is to decide the radiation factor with a suitable method. And the radiation factor could be written as

$$|R_n|^2 = \frac{4}{q^2}\exp(2\,|\gamma_0|\,z_0)(1-\cos^2\eta\sin^2\zeta)^{-1} \times$$

$$\left[\frac{\varepsilon_0}{\mu_0}\left|\varPhi^r_{n,y}(\omega,\beta)\right|^2 + \left|\varPsi^r_{n,y}(\omega,\beta)\right|^2\right], \quad (6)$$

where μ_0 is the permeability of vacuum and $\varPhi^r_n(\omega,\beta)$, $\varPsi^r_n(\omega,\beta)$ are the magnitudes of the reflected field in the frequency domain which are calculated using the

"Modal Expansion Method" (MEM) in this paper. The radiation factor strongly depends on the energy of the electron, on the direction of observation (ζ, η) and on the grating profile. So we can choose the optimized grating profile to achieve the maximum output power. Considering that the grating profile has no influence on the calculation of the coherent factor, we take the single particle emission as the example.

We first assume that the groove width is $A/D=0.5$. Then, we can conclude from Fig. 8 that there are two types of grating that have strong emission power: the shallow grating with $H/D=0.11$ and the deep grating with $H/D=0.9$. For deep grating, the peak of emission power reaches a higher value, but is restricted to a narrow angular interval. However, for shallow grating the emission could be detected in a wide range of angular interval. In conclusion, the two gratings are needed for different experiment schemes.
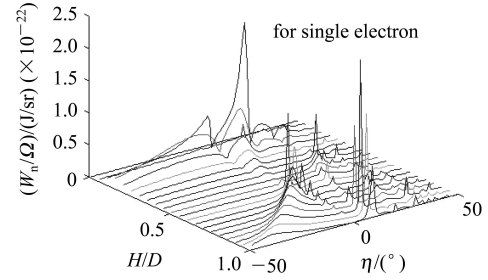

Fig. 8. Emission energy per solid angle for single electron.

For the shallow grating, we seek for wide range angular distribution of radiated energy. Thus, we choose the groove width with $A/D=0.5$, whose energy distribution is wide in both forward and backward direction (see Fig. 9).
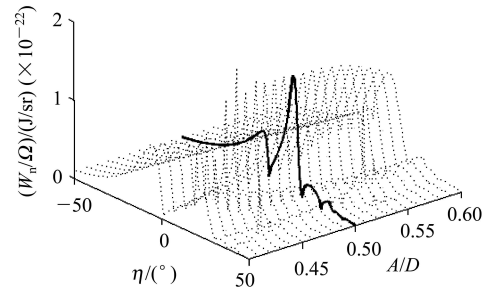

Fig. 9. Emission energy for the shallow grating.

Otherwise, for the deep grating we seek for the higher peak value of radiated energy. As is presented from Fig. 10, we choose the groove width with $A/D=0.685$, whose peak can reach as high as 1.4×10^{-21}(J/sr) enhanced by about ten times compared with the shallow grating.
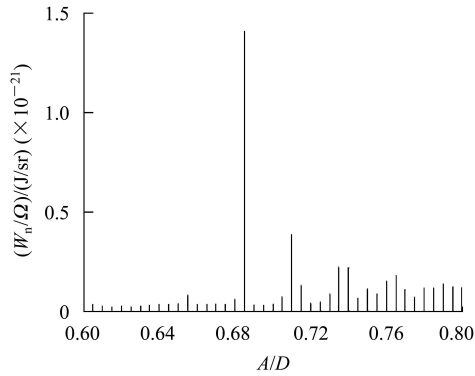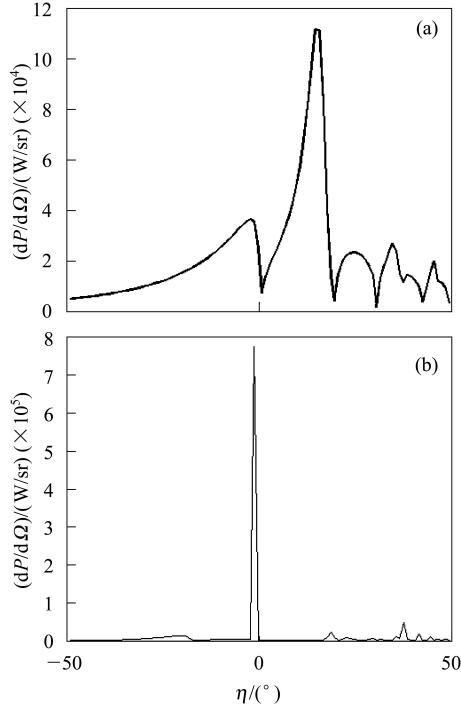
Fig. 10.　Emission energy for the deep grating.

Fig. 11.　Emission power per solid angle for (a) shallow grating and (b) deep grating.

To sum up, the overall parameters for the experiment are listed in Table 2 according to these optimization results.

Table 2.　Parameters for SP-emitter experiment.

quadrupoles strength	
$Q6/(\text{T/m})$	0.1186
$Q7/(\text{T/m})$	-2.0699
grating parameters	
beam-grating distance/μm	360
grating period/μm	369
number of periods	160
groove depth $H/D(S/D)$	0.11/0.9
groove width $A/D(S/D)$	0.5/0.685

Note: S or D represents shallow or deep grating respectively.

Then, the power per unit solid angle for the two types of grating could be calculated using these parameters, as shown in Fig. 11.

4　Detection methods and devices

The radiation could be exported through the quartz window whose attenuation coefficient is already known, and then the gold-coated parabolic mirror is needed to transmit the light to our detector. And we can achieve the angular intensity detection by moving the grating forward or backward using the stepper motor. That could adjust the angle of emission through the quartz window.

The intensity of SP radiation could be detected using a pyroelectric detector which can work at the room temperature. Besides, the power spectrum of the coherent SP radiation could be analyzed using the Michelson interferometer by Fourier transformation of the autocorrelation function.

References

1　Siegel P H. IEEE Trans. on MTT, 2002, **50**: 910
2　Smith S J, Purcell E M. Phys. Rev., 1953, **92**: 1069
3　Doucas G, Kimmitt M F, Andrews H L et al. Phys. Rev., ST Accel. Beams., 2002, **5**: 072802
4　Doucas G, Blackmore V, Ottewell B et al. Phys. Rev. ST Accel. Beams., 2006, **9**: 092801
5　Ishi K, Shibata Y, Takahashi T et al. Phys. Rev. E., 1995, **1**: R5212